Polymorphic estrogen receptor binding site causes CD2-dependent sex bias in the susceptibility to autoimmune diseases

Gonzalo Fernandez Lahore
Karolinska Institute https://orcid.org/0000-0002-4291-0251
Michael Förster
Karolinska Institute
Martina Johannesson
Karolinska Institutet https://orcid.org/0000-0002-4353-7583
Pierre Sabatier
Karolinska Institute https://orcid.org/0000-0002-2734-1791
Erik Lönnblom
Division of Medical Inflammation Research https://orcid.org/0000-0002-1311-2541
Mike Aoun
Karolinska Institute
Yibo He
Karolinska Insitutet
Kutty Nandakumar
Southern Medical University https://orcid.org/0000-0001-7790-8197
Roman Zubarev
Karolinska Institute https://orcid.org/0000-0001-9839-2089
Rikard Holmdahl (rikard.holmdahl@ki.se)
Karolinska Institute https://orcid.org/0000-0002-4969-2576

Article

Keywords: Immunogenetics, Gene regulation, autoimmune diseases, Polymorphic estrogen receptor, CD2

Posted Date: April 2nd, 2021

DOI: https://doi.org/10.21203/rs.3.rs-337166/v1

Version of Record: A version of this preprint was published at Nature Communications on September 22nd, 2021. See the published version at https://doi.org/10.1038/s41467-021-25828-5.

Abstract

Complex autoimmune diseases are sexually dimorphic. An interplay between predisposing genetics and sex-related factors likely determines the sex discrepancy in the immune response, but conclusive evidence is lacking regarding the underlying molecular mechanisms. Using forward genetics, we positionally identified a polymorphic estrogen receptor binding site that regulates *CD2* expression, leading to female-specific differences in mouse models of T cell-dependent autoimmunity. Female mice with reduced CD2 levels displayed diminished expansion of autoreactive T cells. Mechanistically, CD2 affected T cell activation by inhibiting LAG-3 expression. Our findings explain the sexual dimorphism in human autoimmunity, as CD2 associated with rheumatoid arthritis and its regulation through 17-β-estradiol was conserved in human T cells. Hormonal regulation of CD2 has implications for CD2-targeted therapy. Indeed, anti-CD2 treatment was more potent in female mice. In conclusion, our results demonstrate the relevance of sex-genotype interactions and provide strong evidence for CD2 as a sex-sensitive predisposing factor in autoimmunity.

Introduction

Women mount a more vigorous immune response and are more susceptible to most autoimmune diseases [1,2]. These diseases have a strong but complex genetic component, and it has been difficult to identify the underlying polymorphisms [3–5]. The female preponderance in autoimmunity is sex hormone related [6] but could also be genetically dependent [7]. Not only through sex chromosomes but also through distinct sex hormone regulated expression of autosomal genes. However, conclusive evidence is still lacking, as it is difficult to positionally identify the underlying polymorphisms controlling complex traits in a sex-dependent manner.

Analysis of genetically segregated inbred animal strains dramatically enhances the power to isolate polymorphisms underlying complex diseases. Compared with association studies of human cohorts, studies in mice reduce environmental variability and allow for proof-of-concept experiments in biologically relevant systems, making it possible to conclusively identify genes underlying complex traits. In the context of previous such work to identify genetic loci that regulate autoimmune arthritis [8–10], we have identified a locus on mouse chromosome 3 (Cia21) that affects expression of the T cell activation marker *CD2* and regulates arthritis severity in females, but not in males [9]. We herein find the cause of the effect to be a polymorphic estrogen receptor binding site (ERBS) within Cia21 that recapitulates the phenotypic properties of its parent locus. This polymorphic ERBS orchestrates expression of surrounding genes in a sex-specific manner, including CD2. We isolated these polymorphisms in a congenic mouse line (D3-31) and used these mice to study the consequences of estrogen-mediated regulation of CD2 for T cell-dependent autoimmunity. In addition, we found estrogen regulation of CD2 expression to be a conserved mechanism in humans that likely contributes to the sexual dimorphism in T cell-mediated autoimmune diseases.

Results

We have set out to identify major genetic polymorphisms underlying the development of autoimmune arthritis, using animal models. As part of these efforts we previously described a major quantitative trait locus (QTL) on chromosome 3 qF2.2, which we termed Cia21 [9]. Cia21 was identified from an inter-cross between the collagen-induced arthritis (CIA)-susceptible C57BL/10.RIII (BR) and the CIA-resistant RIIIS/J (R3) mouse strains [11]. Cia21 contains several differentially expressed genes, including *CD2* and *PTPN22* [9]. Both CD2 and PTPN22 play a key role in T cell activation and were proposed as strong candidate genes. The aim of the present study is to identify the polymorphisms underlying the Cia21 QTL.

A minimal non-coding genetic interval proximal to CD2 recapitulates the arthritis-regulating properties of Cia21

To dissect the Cia21 QTL, we bred heterozygous Cia21 mice and evaluated the resulting recombinant mice (shown in Fig. 1a) using CIA (Fig. 1b). Out of all the evaluated recombinants, only two, numbers 1 and 5, recapitulated the protective arthritis phenotype previously observed in Cia21 mice [9]. Thus, the Cia21 QTL results from individual contributions of these two sub-QTLs. Importantly, the phenotype driving recombinant regions 1 and 5 mapped to the previously proposed [9] candidate genes *CD2* and *PTPN22*, respectively. Recombinant fragment 1 (proximal to *CD2*), however, was significantly smaller than fragment 5 providing better conditions for the positional identification of underlying polymorphisms. Therefore, we focused our efforts on the former.

Recombinant fragment 1 stretched from markers D3KV1 to MF31 (Fig. 1a, ca. 0.2 Mbp), but could be further redefined to the significantly smaller D3KV1-MF96 interval (ca. 0.02 Mbp) through a recombination assisted breeding strategy. Although recombinant fragments 1, 2, and 3 overlapped significantly, only fragment 1 regulated arthritis. Thus, we concluded that the causative polymorphisms must be positioned between markers D3KV1 and MF96 (Fig. 1a, highlighted yellow). D3KV1-MF96 is a non-coding 0.02 Mbp region proximal to *CD2*, located in-between the genes *ATP1A1* and *IGSF3* (Fig. 1c). We isolated the D3KV1-MF31 recombinant fragment (termed D3-31) in a congenic mouse line for further investigations. D3-31 congenic mice carry the parental R3 allele of D3-31 on an otherwise BR background. For simplicity, we hereon refer to the congenic line as D3-31 and to wild type littermates as BR.

D3-31 congenic mice are protected from several T cell-dependent models of autoimmunity in a sex-specific manner

In accordance with our previous data on Cia21, the R3 allele of D3-31 protected congenic mice in T cell-dependent [12–14] autoimmune inflammatory models, including collagen induced arthritis (CIA), experimental autoimmune encephalomyelitis (EAE), and delayed type hypersensitivity (DTH) (Fig. 2a-f). We also investigated the T cell-independent [15] collagen antibody-induced arthritis (CAIA) model, but observed no phenotypic differences (supplementary fig. S1). As the DTH model does not depend on B

cells [12], these results indicated a critical role for T cells. Interestingly, and as previously described for Cia21 [9], only female D3-31 mice were protected from T cell mediated autoimmunity (Figs. 2a-f). Thus, we concluded that D3-31 regulates T cell dependent autoimmune phenotypes, and likely T cells, in a sex-specific manner.

Female sex hormones are required for the protective phenotype in D3-31 mice

To discriminate between influence of sex chromosomes versus hormones, we performed CIA and EAE experiments in castrated female mice (Fig. 3a-c). Castration of female mice depletes gonadal production of 17-β-estradiol (E2) [16], which constitutes the major circulating estrogenic compound in females. Castration reverted the protective effect of the D3-31 fragment both in CIA and EAE (Fig. 3a-c), which demonstrated the crucial contribution of female sex hormones, most likely E2, to the protective phenotype in female D3-31 mice. We next defined the genetic mechanisms underlying this sexually dimorphic immune phenotype by sequencing the D3-31 fragment.

Polymorphisms in an estrogen receptor binding site (ERBS) affect E2-mediated transcriptional activity

DNA sequencing of the D3-31 BR and R3 alleles revealed four single nucleotide polymorphisms (SNPs) in the critical D3KV1-MF96 interval (Fig. 4a and b). None of the variants affected the coding region of known genes, indicating distal (cis) regulation of gene expression, likely by interfering with regulatory elements. Given our previous observations, we speculated that the identified polymorphisms could be located within an ERBS, interfering with sex-dependent regulation of gene expression.

Estrogen receptors (ERα and ERβ) are nuclear hormone receptors that translate E2-mediated signalling. Both ERα and ERβ are expressed in immune cells [17], and act as transcription factors regulating the expression of proximal and distant genes [18,19]. To test our hypothesis, we screened publicly available ChIP-seq data for ERα binding sites overlapping with one or more of the sequenced SNPs within D3KV1-MF96 interval. Indeed, one of the SNPs, AC > GG on chr3:101310478-479 (termed SNP478), clearly overlapped with an ERα binding site (Fig. 4c). In fact, bioinformatic analysis also revealed an estrogen response element (i.e. an ER core binding motif) in close proximity to SNP478. We sought to verify this finding, and confirmed binding of ERα to SNP478 in spleen cells using ChIP-qPCR (Fig. 4d). Comparison of SNP478 between mouse inbred strains revealed that this SNP is in fact part of a highly polymorphic AC/GT simple repeat (supplementary fig. S2, extracted from [20]).

To address whether SNP478 had functional consequences for E2-mediated transcriptional activity (i.e. interfered with the binding of ERα to the DNA), we cloned the candidate D3KV1 ERBS (± 100 bp) in its two variant forms (AC and GG) into luciferase reporter constructs. We assessed transcriptional activity of these constructs in transfected ERα + MCF-7 cells treated with increasing concentrations of E2 (Fig. 4e). In the context of the reporter construct, an increased occupancy of the ERBS by ERα (as a function of

increasing E2) resulted in suppression of transcriptional activity. Although surprising, similar observations have been reported elsewhere [21]. Given the stronger transcriptional inhibition when using the BR derived construct, we concluded that ERα has a higher affinity for the BR allele than for the D3-31 allele. Importantly, these data demonstrate that SNP478 has functional consequences for E2-mediated transcriptional activity.

Polymorphism in an ERBS leads to female-specific changes in CD2 expression

Next, we tested the biological relevance of our findings by comparing the gene expression profile in lymphoid tissue from male and female D3-31 and BR mice. We observed female-specific changes in the expression of three genes adjacent to the polymorphic ERBS, namely *CD2*, *IGSF3* and *MAB21L3* (Fig. 5a). We also investigated the expression of *ATP1A1* as well as more distal genes (*CD101* and *SLC22A15*) previously implicated in the non-obese diabetic (NOD) mouse model of type 1 diabetes [22], but found no changes in their expression level. Notably, the female-specific reduction of CD2 expression in D3-31 mice was also evident at protein level (Fig. 5b), and correlated with our previously reported gene expression results [9].

Out of the differentially expressed genes, *CD2* was the only gene predominantly expressed in lymphoid tissue (Fig. 5c), particularly in activated $CD4^+$ T cells (Fig. 5d). *IGSF3* and *MAB21L3* regulate neural [23] and ocular [24] development, whereas CD2 has been involved in immune function [25] and associated with human autoimmune conditions [4,26]. Indeed, treatment of lymph node cells with anti-CD2 mAb inhibited T cell activation as demonstrated by reduced secretion of pro-inflammatory cytokines (Fig. 5e). Considering these data and normal development of D3-31 mice, we concluded that CD2 is driving the T cell-dependent immune phenotype observed in D3-31 mice.

Given the sex-specific differences in gene expression, we next investigated the relation between E2 and CD2 expression. T cells cultured in the presence of E2 up-regulated CD2 in a dose-dependent manner (Fig. 5f). Conversely, use of E2 depleted medium (achieved by using charcoal-stripped serum) reduced the expression of CD2, and, more importantly, neutralized the observed differences in CD2 expression between BR and D3-31 mice. Additionally, differences in CD2 expression could be re-established by reintroducing E2 to the medium (Fig. 5g). This not only demonstrates direct regulation of E2 on CD2 expression, but also proves that the identified polymorphisms interfere with this regulation. Consequently, we speculated that E2-mediated regulation of CD2 was contributing to sex-specific differences in the T cell responses. A sex-dependent reduction of CD2 expression in female D3-31 mice could likely limit the T cell responses.

E2-dependent regulation of CD2 expression leads to sex-specific differences in autoreactive T cell activation

To investigate the impact of sex hormone-dependent alterations in CD2 expression on the T cell responses, we compared the activation of T cells between BR and D3-31 female mice. In a first set of *in*

vitro experiments, we found an impaired response in D3-31 T cells to TCR stimulation, as evidenced by reduced proliferation and IL-2 production (Fig. 6a). Importantly, the difference in T cell proliferation between BR and D3-31 mice could be enhanced in a dose-dependent manner by E2 (Fig. 6b), much like the E2-dependent expression differences observed for CD2 (Fig. 5g).

A diminished T cell response in D3-31 mice was also evident *in vivo*. Compared to BR mice, D3-31 mice showed a lower level of antigen specific T cells responses 10 days after immunization with CIA antigen bovine collagen type II, as demonstrated by reduced secretion of proinflammatory cytokines in lymph node cultures recalled with antigen (Fig. 6c). Flow cytometry analysis of D3-31 draining lymph nodes revealed lower numbers of antigen experienced $CD40L^+$ $CD4^+$ T cells (Fig. 6d), which expressed reduced levels of CD2 and L-17A after *ex vivo* restimulation with PMA (Fig. 6d and e). Differences in T cell activation status were also evident by lower numbers of induced regulatory T cells after immunization (Fig. 6f). Importantly, the observed differences in T cell activation were strictly sex-specific (Fig. 6d-f), mirroring sex-specific differences in CD2 expression. Treatment with anti-CD2 strongly reduced the expression of IL-17 in naïve and autoreactive $CD4^+$ T cells (Fig. 6g and e, respectively), as well as FOXP3 in naïve T cells (Fig. 6g), demonstrating a key role for CD2 in the differentiation of Th17 and Treg cells. Consequently, we concluded that reduced CD2 expression in female D3-31 mice limits T cell activation in a sex-specific manner.

Although CD2 can regulate TCR signalling by increasing the stability of the immune synapse, we thought it plausible that persistent differences in CD2 signalling could elicit more profound phenotypic changes. Proteomic and flow cytometric analysis of $CD4^+$ T cells treated with an anti-CD2 mAb resulted in a selective up-regulation of the immune inhibitory marker LAG-3 (Fig. 6h). Thus, our data suggests that CD2 signalling modulates T cell activation not only by stabilizing the immune-synapse, but also by regulating the expression of the inhibitory marker LAG-3.

CD2 associates with rheumatoid arthritis (RA) and is regulated by E2 in humans

Our results in mice suggested a regulatory role for *CD2* on T cell-dependent autoimmunity, which is genetically determined in a sex-linked manner. We therefore explored the relevance of our findings in humans in the context of RA. In a genetic association study, we found a significant association between *CD2* polymorphisms and RA (Fig. 7a). While this association was more often found in females than in males, this was likely due to higher prevalence of RA in females (female to male ratio 3:1). Interestingly, several of the SNPs associated with RA ($p < 0.05$) can enhance expression of *CD2* (Fig. 7b), as we determined from the GTEx database [27]. Further analysis of available microarray datasets [28] revealed a mild yet significant correlation between *CD2* expression in RA synovia and disease activity (Fig. 7c). Moreover, *CD2* is strongly up-regulated in the synovial tissue from RA patients when compared to osteoarthritis or healthy synovium (Fig. 7d). Thus, it is likely that CD2 is involved in joint inflammation, and that *CD2* polymorphisms affecting its expression contribute to the development or perpetuation of joint autoimmunity.

Importantly, women expressed higher levels of *CD2* than men, both in RA synovium and healthy PBMCs (Fig. 7c and 7e, respectively), suggesting the E2-mediated regulation of *CD2* observed in mice is conserved in humans as well. To corroborate our findings, we stimulated $CD4^+$ T cells from healthy human donors with increasing amounts of E2. Firstly, we noticed a strong up-regulation of CD2 in antigen experienced $CD45RO^+$ T cells compared to their naïve $CD45RA^+$ counterparts (Fig. 7f). But more importantly, expression of CD2 could be enhanced in $CD45RO^+$ T cells by incubation with E2 in a concentration-dependent manner (Fig. 7g). Indeed, analysis of available ChIP-seq data [29] revealed that ERα robustly binds the human *CD2* gene locus (Fig. 7h). Thus, these data demonstrate the evolutionary conserved nature of E2-mediated regulation of CD2.

We reasoned that hormonal regulation of CD2 expression could have implications for anti-CD2-mediated therapy, as previous research suggests that anti-CD2 (Alefacept) preferentially targets $CD2^{hi}$ T cells [30]. To test this, we compared the *in vivo* effects of anti-CD2 mAb administration on circulating T cells from male and female mice (Fig. 7i). Anti-CD2 mAb treatment partially depleted circulating T cells, and resulted in the relative enrichment of remaining effector $CD44^+$ T cells, skewing the naïve $CD62L^+$/effector $CD44^+$ T cell ratio. This effect was significantly more pronounced in females, which, like in humans, expressed higher levels of CD2 in circulating T cells. Taken together, these data demonstrate that sex-dependent differences in CD2 expression determine the response to anti-CD2 mAb.

Discussion

Using forward genetics, we have positionally identified a polymorphic ERBS regulating T cell-dependent autoimmunity. This site orchestrates expression of surrounding genes in a sex-specific manner, including expression of the T cell co-stimulatory molecule, CD2. We find that E2-mediated regulation of CD2 is a conserved mechanism that influences T cell activation in a sex-specific manner, contributing to the sexual dimorphism in autoimmune diseases.

Understanding the sexual dimorphic immune responses is fundamental for personalized medicine but is methodologically challenging. Common approaches to study this phenomenon rely on intricate manipulation of gonadal or hormonal systems [31], which has yielded valuable insights but with limited physiological relevance. Our study provides a more physiological perspective by the identification of a naturally occurring polymorphism in an ERBS, which enables studies on sex-associated differences in T cell-mediated autoimmunity. Since we used a hypothesis-free approach, our findings strongly suggest E2-mediated regulation of CD2 as a key physiological mechanism contributing to sex differences in the T cell responses and susceptibility to autoimmunity.

Our results also highlight the importance of genotype-sex interactions for the sexual dimorphism in autoimmune diseases. While much attention has been devoted to the contribution of sex chromosomes, epigenetic mechanisms or direct actions of hormones to the sexually dimorphic immune responses, the interactions between sex and predisposing autosomal polymorphisms have remained elusive. Isolated studies have demonstrated sex-dependency of expression (e) QTLs [32] and sex differences in the genetic

associations to inflammatory diseases [33–35], but evidence is limited. Using a hypothesis-free approach, we for the first time conclusively identify a sex biased QTL with direct consequences for the development of autoimmunity. Polymorphisms in the identified ERBS modulate E2-driven CD2 expression, leading to sex-specific differences in T cell autoimmunity. Our results demonstrate not only that genetic polymorphisms influence hormonal regulation of gene expression, but also that genotype-sex interactions shape the sexually dimorphic immune response.

Independent of our sex-related findings, this study provides valuable insights into CD2 immunobiology. Polymorphisms in the *CD2* locus have been previously associated with several autoimmune diseases [4,26], but not much attention was given to the mechanism of action of these polymorphisms. Similarly, CD2 has been explored as a therapeutic target, but its mechanism of action beyond depletion of circulating T cell is poorly characterised [36], and complex adverse effects (including malignancies [37]) warrant further research. CD2 in isolation affects the formation of the immune synapse [3839] and T cell activation [4041], but the relevance of these findings *in vivo* are less clear. For example, targeting CD2 in mice does not seem to affect immune system development [42] or thymic T cells [43], unless TCR transgenic systems are used [4445]. Thus, there is a need to study this therapeutically promising pathway in a physiologically relevant context. The D3-31 mice used in this study exhibit discrete changes in CD2 expression mediated by E2, thus enabling us to study the effect of CD2 on T cell mediated autoimmunity in a physiological setting.

We show for the first time that changes in CD2 expression, caused by natural polymorphisms, affect the T cell responses. Reduced CD2 expression protected mice from T cell-dependent inflammation and autoimmunity by reducing the activation and proliferation of antigen-specific T cells. This is consistent with studies demonstrating that CD2 membrane density is proportional to TCR signalling strength [38], and that peptide-based blocking of CD2 signalling reduces CIA severity [46]. Our results also implicate CD2 in the generation of Th17 and Treg- type T cell responses. Mice with reduced CD2 expression had a diminished T cell response characterized by a reduced expansion of Th17 and Treg cells. Accordingly, blocking CD2 resulted in the suppression of both cell types *in vitro*. Indeed, CD2 has been linked to Treg [47,48] and Th17 phenotypes [39] before, and targeting CD2 is effective in the treatment of Th17-mediated inflammatory diseases like psoriatic arthritis [49]. In summary, this suggests a key role for CD2-mediated activation in the induction of Th17 and Treg cells.

Mechanistically, CD2 seems to play a role in T cell activation beyond its ability to stabilize the immune synapse, as blocking CD2 results in selective up-regulation of the exhaustion marker, LAG-3. This finding is supported by studies showing an inverse correlation between CD2 expression and exhaustion of T cells [38 50], and up-regulation of LAG-3 in human CD8 T cells after treatment with Alefacept (anti-CD2) [51]. Thus, together with other studies, our data suggests that CD2 signalling maintains T cell autoreactivity by reducing the expression of inhibitory LAG-3 molecule.

Our findings in mice are likely relevant to the sexual dimorphism observed in human autoimmune conditions. *CD2* associates with RA and E2 regulation of CD2 expression is highly conserved in human T cells. Women, who are generally more prone to autoimmunity, express higher levels of *CD2* than men. In mice, we demonstrate that these type of discrete and sex-specific differences in CD2 expression result in sexually dimorphic T cell responses and autoimmune phenotypes. Thus, subtle, physiological changes in CD2 expression caused by natural polymorphisms likely modify the risk of T cell-dependent autoimmunity in humans. E2-mediated regulation of CD2 probably contributes to sex differences in the immune responses, both in homeostasis as well as autoimmune conditions.

Sex-dependent differences in CD2 expression have implications for several sexually dimorphic immune processes involving T or other CD2 expressing cells. Hormonal regulation of CD2 could contribute to more vigorous humoral immune responses in women [2], helping to protect their off-spring from infections [52] at the cost of an enhanced risk to autoimmunity post-partum [53]. Alternatively, an enhanced CD2 expression in women might facilitate the induction of regulatory T cell phenotypes (as we observed in mice) to facilitate foetal-maternal immune tolerance. A hormonal regulation of CD2 expression could have wide ranging implications for the personalized therapy of T cell-mediated inflammatory diseases, as Alefacept was shown to preferentially target $CD2^{hi}$ T cells [30]. Indeed, we demonstrate strong effects of anti-CD2 mAb administration on the naïve/effector T cell ratio in female, but not male mice. As such, sex-specific differences in T cell CD2 expression may offer a useful biomarker for stratification of patients in the context of CD2 targeted therapies.

In conclusion, our results highlight the importance of genotype-sex interactions for the sexual dimorphism in autoimmunity, demonstrating that sex can determine the penetrance of predisposing genetic factors. Our findings show that CD2 is a sex-sensitive regulator of T cell-mediated autoimmunity. Hormonal regulation of CD2 is a conserved mechanism that has implications for the sexual dimorphism in the susceptibility to -and treatment of- autoimmune diseases like RA.

Materials And Methods

Animals. The BR.Cia21.D3-31 congenic founder mice were obtained from a partial advanced intercross (PAI) described elsewhere and they were subsequently back crossed for four additional generations [9]. In order to ensure strain purity, BR.Cia21.D3-31 mice were screened with a custom designed 8k Illumina chip at genome wide level [54] and the mice were found to be devoid of any contaminating RIIIS/J alleles. No SNPs were present between the congenic and the B10.RIII background strain. Mice were kept under specific pathogen free (SPF) conditions in the animal house of the Section for Medical Inflammation Research, Karolinska Institute in Stockholm. Animals were housed in individually ventilated cages containing wood shavings in a climate-controlled environment with a 14 h light-dark cycle, fed with standard chow and water *ad libitum*. All the experiments were performed with age-, sex- and cage-matched mice and all the genetic experiments were performed with littermate controls. All the

experimental procedures were approved by the ethical committees in Stockholm, Sweden with ethical permit numbers; 12923/18 and N134/13 (genotyping and serotyping), N35/16 (CIA) and N83/13 (EAE).

Preparation of mouse single cell suspensions. Briefly, spleen or lymph nodes were harvested and mechanically dissociated on a 40 µM cell strainer (Falcon) using a 1ml syringe plunger (Codan). Cells were counted on a Sysmex KX-21 cell counter. All centrifugation steps throughout the study were carried out a 350 x g for 5 min at RT. For spleen samples, red blood cells were lysed in RBC buffer (155 mM NH4Cl, 12 mM NaHCO3, 0.1 mM EDTA) before counting.

Preparation of human peripheral blood mononuclear cells (PBMC). Human PBMCs were prepared from 8 ml whole blood of healthy donors using SepMate (Stemcell Technologies) tubes and Ficoll density gradient medium (Sigma) according to the manufacturer. Ethical permit number: Dnr 2020–05001.

Cell culture. 10^6 splenocytes, 5×10^5 lymph node cells, or 10^5 PBMCs were cultured in 200 µl of complete RPMI per well in Nunclon U-shaped bottom 96-well plates (Thermo Scientific). Cells were incubated at 37°C and 5% CO_2. Complete RPMI: RPMI 1640 with GlutaMAX™ (Thermo Scientific); 10% heat inactivated FBS (Thermo Scientific); 10 µM HEPES (Sigma); 50 µg/ml streptomycin sulfate (Sigma); 60 µg/ml penicillin C (Sigma); 50 µM β-Mercaptoethanol (Thermo Scientific). FBS was heat-inactivated for 30 min at 56°C. To assess the effect of 17-β-estradiol (Sigma) on CD2 expression, the medium was supplemented with charcoal-stripped FBS instead (Thermo Scientific). 17-β-estradiol was solved in ethanol.

ELISA. 10^6 lymph node cells from CIA mice were plated per well and stimulated with 100 µg/ml bovine collagen type II (bCII) in complete RPMI for 48 h as described in *cell culture*. Supernatants were used for cytokine analysis. Flat 96-well plates (Maxisorp, Nunc) were coated overnight at 4°C with the capture antibody (Ab, listed below) in PBS. After removing the coating solution, supernatant from cell cultures were added. Plates were incubated for 3 h at RT before washing (0.05% Tween PBS) and adding the biotinylated detection Ab (listed below) in PBS (1 h at RT). Plates were washed and incubated 30 min at RT with Eu-labelled streptavidin (PerkinElmer, 1:1000) in 50 mM Tris-HCl, 0.9% (w/v) NaCl, 0.5% (w/v) BSA and 0.1% Tween 20, 20 µM EDTA. After washing, DELFIA Enhancement Solution (PerkinElmer) was added and fluorescence read at 620 nm (Synergy 2, BioTek). Monoclonal antibodies (mAbs) to IL-2 (capture Ab 5 µg/ml JES6-IA12; detection Ab 2 µg/ml biotinylated-JES6-5H4, in-house produced), IL-17A (capture Ab 5 µg/ml TC11-18H10.1; detection Ab 2,5 µg/ml TC11-8H4, Biolgend), IFN-γ (capture Ab 5 µg/ml AN18; detection Ab 2,5 µg/ml biotinylated R46A2, in-house produced).

Analysis of mRNA expression. 10^6 lymph node cells per well were stimulated for 24 h using mAb LEAF hamster anti-mouse CD3 (1 µg/ml, 500A2, BD Pharmingen) and LEAF hamster anti-mouse CD28 (1 µg/ml, 37.51, BD Pharmingen) as described in *cell culture*. Cells were washed in PBS and RNA was extracted using Qiagen RNeasy columns according to the manufacturer without DNAse digestion. RNA concentration was determined using a NanoDrop 2000 (Thermo Scientific). Sample concentrations were normalized before proceeding with reverse transcription. Samples were stored at -20°C for short-term

storage. cDNA synthesis was carried out using the iSrcipt cDNA synthesis kit (Bio-Rad) according to the manufacturer. qRT-PCR primers covered an exon-exon junction to minimize amplification of genomic DNA and were used at a final concentration of 300 nM. The qPCR reaction was carried out using the iQSYBR Green Mix (Bio-Rad) in white 96-well plates (Bio-Rad) using a CFX96 real-time PCR detection system (Bio-Rad). *ACTB* or *GAPDH* were used as an internal control. Primer sequences are listed in supplementary table 2. Data were analysed according to the ΔΔCt method [55], assuming equal efficiency for all the primer pairs.

ChIP-qPCR. $10x10^6$ spleen cells/ml were fixed for 10 min in 1% formaldehyde PBS at RT. The reaction was stopped by adding 125 mM glycine and cells were washed twice in ice-cold PBS. Complete protease inhibitor cocktail (Roche) was added in all the following steps. $2x10^6$ cells were lysed in 1 ml cell lysis buffer [56] on ice for 15 min, and the extracted nuclei lysed in 1 ml nuclear lysis buffer [56] on ice for 15 min. Lysates were sonicated for 15 cycles (on high settings, 30”ON-30”OFF) using a Diagenode Bioruptor. The water bath was cooled to 4°C before beginning sonication. Average DNA length after sonication was 500 bp. 450 µl of the lysates were incubated with 10 µg/ml rabbit anti-mouse ERα Ab (clone E115, Abcam) or polyclonal rabbit IgG isotype control (Abcam) on a shaker at 4°C over night. Next day, DNA-Ab complexes were precipitated using protein G magnetic beads (Thermos Scientific). Beads were washed twice for 5 min at RT in buffers of increasing salt concentration according to [56]. DNA was eluted by incubating beads in 100 µl elution buffer [56] at 65°C for 30 min with occasional vortex. Beads were pelleted and fixation was reversed by incubation of supernatants for 8 h at 65°C in the presence of 0.3 M NaCl in 96-well plates. On the third day, 10 µg/ml RNAse A (Thermo Scientific) was added for 30 min (37°C) before incubation with 10 µg/ml of Proteinase K (Thermo Scientific) at 55°C for 30 min. DNA was purified using GeneJET PCR purification kit (Thermo Scientific) and used for qPCR. Primers used for amplification of recovered DNA are listed in supplementary table 3. Data was analysed according to [56], but briefly, results are presented as fold change over their respective mock IP controls.

Flow cytometry. 10^6 cells were blocked in 20 µl of PBS containing 5 µg in-house produced 2.4G2 in 96-well plates for 10 min at RT. Samples were washed with 150 µl of PBS and subsequently stained with the indicated antibodies in 20µl of PBS diluted 1:100 or 1:200 at 4°C for 20 min in the dark (Ab list follows). Cells were washed once, fixed and permeabilized for intracellular staining using BD Cytofix/Cytoperm™ (BD) according to the manufacturer. Cells were stained intracellularly with 20 µl of permeabilization buffer (BD), using the antibodies at a 1:100 final dilution, for 20 min at RT. FOXP3 staining required nuclear permeabilization and was carried out using Bioscience™ FOXP3/Transcription Factor Staining Buffer. For intracellular cytokine staining, cells were stimulated *in vitro* with phorbol 12-myristate 13-acetate (PMA) 10 ng/ml, ionomycin 1 µg/ml, and BFA 10 µg/ml for 4–6 h at 37°C prior to fixation, permeabilization and staining.

Flow cytometry anti-mouse antibodies (BD Pharmingen): CD3 (clone: 145-2C11); TCRB (H57-597); CD4 (RM4-5); CD8 (53 – 6.7); CD19 (1D3, 6D5); CD11B (M1/70); CD11C (HL3, N418); FOXP3 (FJK-16s); CD25

(7D4); CD44 (IM7); CD62L (MEL-14); CD2 (RM2-5); LY6C (AL-21); LAG-3 (C9B7W); CD40L (MR1); IFN-γ (R46A2); IL-17A (TC11-18H10.1). CD16/CD32 (2.4G2, in house).

Flow cytometry anti-human antibodies (BD Pharmingen): CD45 (clone: HI30); CD2 (RPA-2,10); TCRB (IP26); CD4 (OKT4); CD45RA (HI100); CD45RO (UCHL1).

Proliferation assay. 10^7 lymph node cells were labelled using CellTrace™ Violet Cell Proliferation Kit (ThermoFisher Scientific) according to the manufacturer. $5x10^5$ naïve lymph node cells were cultured per well in U 96-well plates as described under *cell culture* in the presence of hamster anti-mouse CD3 (1 µg/ml, 500A2, BD Pharmingen) and hamster anti-mouse CD28 (1 µg/ml, 37.51, BD) for 72–96 h. Proliferation by dilution of CTV was assessed using flow cytometry. Complementary antibody staining was done as described under *flow cytometry*. Proliferation parameters were analysed and calculated using FlowJo 8.8.7.

Collagen-induced arthritis (CIA). 12-week-old mice were immunized with 100 µg of bovine collagen type II (bCII) in 100 µl of a 1:1 emulsion with CFA (BD) and PBS intradermally at the base of the tail. Mice were challenged at day 35 with 50 µg of bCII in 50 µl of IFA (BD) emulsion. Mice were monitored for arthritis development as described in [57]. In short, each visibly inflamed (i.e. swollen and red) ankle or wrist was given 5 points, whereas each inflamed knuckle and toe joint was given 1 point each, resulting in a total of 60 possible points per mouse and day.

Collagen antibody-induced arthritis (CAIA). CII-specific antibodies (M2139, CIIC1, CIIC2 and UL1) were generated and purified as previously described [15]. The sterile cocktail of M2139, CIIC1, CIIC2 and UL1 mAbs (4 mg per mouse) was injected intravenously. On day 7, lipopolysaccharide (O55:B5 LPS from Merck; 25 µg in 200 µl per mouse) was injected intraperitoneally to all mice to increase severity of the disease. Mice were scored as described for CIA.

Experimental induced autoimmune encephalomyelitis (EAE). 12-week-old mice were immunized with a 100 µl emulsion of 250 µg myelin basic protein peptide (MBP) 89–101 peptide in PBS and 50 µl IFA (incomplete Freud's adjuvant) containing 50 µg *Mycobacterium tuberculosis* H37RA (BD). Animals were boosted with 200 ng of *Bordetella pertussis* toxin (Sigma Aldrich, St. Louis, MO, USA) i.p. on day 0 and 48 h post initial immunization. EAE severity was evaluated as described in [58]. Briefly, mice were scored as follows: 0, no clinical signs of disease; 1, tail weakness; 2, tail paralysis; 3, tail paralysis and mild waddle; 4, tail paralysis and severe waddle; 5, tail paralysis and paralysis of one limb; 6, tail paralysis and paralysis of two limbs; 7, tetraparesis; 8, moribund or deceased.

Delayed type hypersensitivity (DTH). Hypersensitivity reaction was elicited by initially immunizing mice with 100 µg bCII emulsified in 50 µl CFA (Difco, Detroit, MI, USA). Ten days later mice were challenged with an injection of 10 µg bCII in 10 mM acetic acid into the dorsal part of the right ear and vehicle control in the left one. Ear swelling was assessed 48 and 72 h later using a calliper.

Ovariectomy. In brief, ovaries of female mice were removed after a single incision through the back skin and bilateral flank incision through the peritoneum. Thereafter, mice were rested for a minimum of 14 days prior to immunization for EAE or CIA as described elsewhere.

Luciferase reporter assay. 2x10^4 MCF-7 cells were seeded into flat 96-well flat bottom plates (Thermo Scientific) and left to adhere overnight. Then cells were transfected with pGL4.17 (Promega) luciferase reporter construct containing the BR or R3 allele of the candidate ERBS (pGL4.17.BR and pGL4.17.R3, respectively). ERBS cloning primers 5'-3', Fw: AGATCTCGAGGGGGAAAGCTCTGACTTGGG; Rv: GTCAAGCTTGAGAAAGAATTTTGCTTATTTAGTCC. Cells were transfected in OPTIMEM medium (Thermo Scientific) using lipofectamine 3000 (Thermo Scientific) according to the manufacturer. The transfection mix (per well) contained 400 ng plasmid, 0.3 µl lipofectamine, and 0.2 µl P3000 reagent. Respective stimuli (20 ng/ml PMA, 10–100 nM E2) were added after 24 h, and cells were further incubated overnight before lysis. Luciferase activity was measured using Pierce Firefly Luc One-Step Glow Assay Kit (Thermo Scientific) in a Synergy-2 plate reader (BioTek).

Genetic association study. Data for genetic variations within CD2-CD58 locus was extracted from previous Immunochip data published elsewhere (PMID: 23143596). After filtering these data correspond to 263 SNPs in 1940 healthy controls (M/F 524/1416) and 2762 RA patients (M/F 817/1945) from the Swedish EIRA study. Association was analysed by PLINK separately for female and male individuals.

Analysis of public microarray expression data. Microarray data was extracted from NCBI GEO Database [28] and analysed using Shiny GEO [59]. GEO accession number is cited wherever NCBI GEO data has been used.

Statistical analysis. Statistical analysis was performed using GraphPad Prism v6.0 or higher. Statistical comparison of two unpaired groups was carried out using Mann-Whitney U non-parametric test. CIA and EAE disease curves were compared using two-way ANOVA multiple comparisons test. P-values under 0.05 were considered statistically significant and are denoted with the symbol *. P-values under 0.01 are denoted **.

Proteomic analysis of enriched CD4 $^+$ T cells. $CD4^+$ T cells were enriched from naïve spleens using untouched $CD4^+$ T cell mouse kit (Dynabeads, Life Technologies). 96-well U bottom plates were pre-coated with 1 µg/ml of anti-CD3 and 1 µg/ml of anti-CD2 in PBS for 3 h at 37°C. 2.5x10^5 $CD4^+$ T cells were plated on the pre-coated plates and cultured for 48 h.

Cell pellets were lysed in a buffer consisting of 1% SDS, 8 M urea and 20 mM EPPS pH 8.5 and sonicated using a Branson probe sonicator (3 s on, 3 s off pulses, 45 s, 30% amplitude). Protein concentration was measured using BCA assay and subsequently 50 µg of protein from each sample were reduced with 5 mM DTT at RT for 45 min followed by alkylation with 15 mM IAA in the dark at RT for 45 min. The reaction was quenched by adding 10 mM DTT and the samples were precipitated using methanol-chloroform mixture. Dried protein pellets were dissolved into 8 M urea, 20 mM EPPS pH 8.5. EPPS (20

mM, pH 8.5) was added to lower the urea concentration to 4 M and LysC digestion was done at a 1:100 ratio (LysC/protein, w/w) overnight at RT. Then urea concentration was lowered to 1 M and trypsin digestion was conducted at a 1:100 ratio (Trypsin/protein, w/w) at RT for 5 h. TMTpro plex (Thermo Fischer Scientific) reagents were dissolved into dry acetonitrile (ACN) to a concentration of 20 µg/µl and 200 µg were added to each sample. The ACN concentration in the samples was adjusted to 20% and the labelling was conducted at RT for 2 h and quenched with 0.5% hydroxylamine (ThermoFischer Scientific) for 15 min at RT. The samples were then combined and dried using Speedvac to eliminate the ACN. Then samples were acidified to pH < 3 using TFA and desalted using SepPack (Waters). Lastly, peptide samples were dissolved into 20 mM NH4OH and 150 µg of each sample was used for off-line fractionation.

Samples were fractionated off-line in a high-pH reversed-phase manner using an UltimateTM 3000 RSLCnano System (Dionex) equipped with a XBridge Peptide BEH 25 cm column of 2.1 mm internal diameter, packed with 3.5 µm C18 beads having 300 Å pores (Waters). The mobile phase consisted of buffer A (20 mM NH_4OH) and buffer B (100% ACN). The gradient started from 1% B to 23.5% in 42 min, then to 54% B in 9 min, 63% B in 2 min and stayed at 63% B for 5 min and finally back to 1% B and stayed at 1% B for 7 min. This resulted in 96 fractions that were concatenated into 24 fractions. Samples were then dried using Speedvac and re-suspended into 2% ACN and 0.1% FA prior to LC-MS/MS analysis.

Peptides were separated on a 50 cm EASY-spray column, with a 75 µm internal diameter, packed with 2 µm PepMap C18 beads, having 100 Å pores (Thermo Fischer Scientific). An UltiMate™ 3000 RSLCnano System (Thermo Fischer Scientific) was used that was programmed to a 91 min optimized LC gradient. The two mobile phases consisted of buffer A (98% milliQ water, 2% ACN and 0.1% FA) and buffer B (98% ACN, 2% milliQ water and 0.1% FA). The gradient was started with 4% B for 5 min and increased to 26% B in 91 min, 95% B in 9 min, stayed at 95% B for 4 min and finally decreased to 4% B in 3 min and stayed at 4% B for 8 more min. The injection was set to 5 µL corresponding to approximately 1 µg of peptides.

Mass spectra were acquired on a Q Exactive HF mass spectrometer (Thermo Fischer Scientific). The Q Exactive HF acquisition was performed in a data dependent manner with automatic switching between MS and MS/MS modes using a top-17 method. MS spectra were acquired at a resolution of 120,000 with a target value of 3.10^6 or maximum integration time of 100 ms. The m/z range was from 375 to 1500. Peptide fragmentation was performed using higher-energy collision dissociation (HCD), and the normalized collision energy was set at 33. The MS/MS spectra were acquired at a resolution of 60,000 with the target value of 2.10^5 ions and a maximum integration time of 120 ms. The isolation window and first fixed mass were set at 1.6 m/z units and m/z 100, respectively.

TMT-10 labelling quantification

Protein identification and quantification were performed with MaxQuant software (version 1.6.2.3). MS2 was selected as the quantification mode and masses of TMTpro labels were added manually and selected as peptide modification. Acetylation of N-terminal, oxidation of methionine and deamidation of asparagine and glutamine were selected as variable modifications while carbamidomethylation of the

cysteine was selected as fixed modification. The Andromeda search engine was using the UP000000589_Mus musculus database (22129 entries) with the precursor mass tolerance for the first searches and the main search set to 20 and 4.5 ppm, respectively. Trypsin was selected as the enzyme, with up to two missed cleavages allowed; the peptide minimal length was set to seven amino acid. Default parameters were used for the instrument settings. The FDR was set to 0.01 for peptides and proteins. “Match between runs” option was selected with a time window of 0.7 min and an alignment time window of 20 min.

Declarations

Acknowledgments

We would like to thank Dr Leonid Padyukov and the EIRA study group for providing the genetic data.

Funding

This work was supported by grants from the Knut and Alice Wallenberg Foundation, the Swedish Association against Rheumatism, the Swedish Medical Research Council, the Swedish Foundation for Strategic Research and Karolinska Institute-KID.

Author contributions

G.F.L. wrote the manuscript with the help of M.F. and R.H. G.F.L. designed, performed, analysed, and interpreted most experiments. M.F. and M.J. designed, performed, and analysed all the experiments shown in figs. 1b, 2 and 3. R.Z. and P.S. performed and analysed experiments requiring mass spectrometry (fig. 6h). K.S.N. helped secure funding and reviewed the manuscript. E.L., M.A., and Y.H. helped with data collection, analysis and interpretation. All authors revised and approved the manuscript. R.H. initiated, designed, and supervised the project and takes overall responsibility for the data.

Competing interest

The authors declare no competing interests.

Data availability

The mass spectrometry proteomics data were deposited to the ProteomeXchange Consortium via the PRIDE partner repository [60] with the dataset identifier PXD024126.

References

1. Billi, A. C., Kahlenberg, J. M. & Gudjonsson, J. E. Sex bias in autoimmunity. *Current opinion in rheumatology* (2019) doi:10.1097/BOR.0000000000000564.

2. Klein, S. L. & Flanagan, K. L. Sex differences in immune responses. *Nature Reviews Immunology* (2016) doi:10.1038/nri.2016.90.
3. Ye, J., Gillespie, K. M. & Rodriguez, S. Unravelling the roles of susceptibility loci for autoimmune diseases in the post-GWAS era. *Genes* (2018) doi:10.3390/genes9080377.
4. Okada, Y., Eyre, S., Suzuki, A., Kochi, Y. & Yamamoto, K. Genetics of rheumatoid arthritis: 2018 status. *Annals of the Rheumatic Diseases* (2019) doi:10.1136/annrheumdis-2018-213678.
5. Bogdanos, D. P. *et al.* Twin studies in autoimmune disease: Genetics, gender and environment. *Journal of Autoimmunity* (2012) doi:10.1016/j.jaut.2011.11.003.
6. Jansson, L. & Holmdahl, R. Estrogen-mediated immunosuppression in autoimmune diseases. *Inflammation Research* (1998) doi:10.1007/s000110050332.
7. Ober, C., Loisel, D. A. & Gilad, Y. Sex-specific genetic architecture of human disease. *Nature Reviews Genetics* (2008) doi:10.1038/nrg2415.
8. Ahlqvist, E., Bockermann, R. & Holmdahl, R. Fragmentation of two quantitative trait loci controlling collagen-induced arthritis reveals a new set of interacting subloci. *J. Immunol.* **178**, 3084–90 (2007).
9. Johannesson, M. *et al.* Identification of epistasis through a partial advanced intercross reveals three arthritis loci within the Cia5 QTL in mice. *Genes Immun.* **6**, 175–185 (2005).
10. Vingsbo-Lundberg, C. *et al.* Genetic control of arthritis onset, severity and chronicity in a model for rheumatoid arthritis in rats. *Nat. Genet.* (1998) doi:10.1038/3887.
11. Johannesson, M. *et al.* Gene expression profiling of arthritis using a QTL chip reveals a complex gene regulation of the Cia5 region in mice. *Genes Immun.* **6**, 575–83 (2005).
12. Taube, M. & Carlsten, H. Cutaneous delayed type hypersensitivity in SCID mice adoptively transferred with lymphocytes is B cell independent and H-2 restricted. *Scand. J. Immunol.* (1997) doi:10.1046/j.1365-3083.1997.d01-433.x.
13. Divya Jyothi, M., Flavell, R. A. & Geiger, T. L. Targeting autoantigen-specific T cells and suppression of autoimmune encephalomyelitis with receptor-modified T lymphocytes. *Nat. Biotechnol.* (2002) doi:10.1038/nbt758.
14. Liu, Y. *et al.* Neuronal IFN-beta-induced PI3K/Akt-FoxA1 signalling is essential for generation of FoxA1 + Treg cells. *Nat. Commun.* (2017) doi:10.1038/ncomms14709.
15. Nandakumar, K. S., Bäcklund, J., Vestberg, M. & Holmdahl, R. Collagen type II (CII)-specific antibodies induce arthritis in the absence of T or B cells but the arthritis progression is enhanced by CII-reactive T cells. *Arthritis Res. Ther.* **6**, R544–R550 (2004).
16. Ding, L. C. *et al.* Rcan2 and estradiol independently regulate body weight in female mice. *Oncotarget* (2017) doi:10.18632/oncotarget.18259.
17. Khan, D. & Ansar Ahmed, S. The Immune System Is a Natural Target for Estrogen Action: Opposing Effects of Estrogen in Two Prototypical Autoimmune Diseases. *Front. Immunol.* **6**, 635 (2015).
18. Carroll, J. S. *et al.* Chromosome-wide mapping of estrogen receptor binding reveals long-range regulation requiring the forkhead protein FoxA1. *Cell* (2005) doi:10.1016/j.cell.2005.05.008.

19. Carroll, J. S. *et al.* Genome-wide analysis of estrogen receptor binding sites. *Nat. Genet.* (2006) doi:10.1038/ng1901.
20. Kent, W. J. *et al.* The Human Genome Browser at UCSC. *Genome Research* vol. 12 996–1006 (2002).
21. Yao, Y., Brodie, A. M. H., Davidson, N. E., Kensler, T. W. & Zhou, Q. Inhibition of estrogen signaling activates the NRF2 pathway in breast cancer. *Breast Cancer Res. Treat.* (2010) doi:10.1007/s10549-010-1023-8.
22. Rainbow, D. B. *et al.* Evidence that Cd101 Is an Autoimmune Diabetes Gene in Nonobese Diabetic Mice. *J. Immunol.* **187**, 325–336 (2011).
23. Usardi, A., Iyer, K., Sigoillot, S. M., Dusonchet, A. & Selimi, F. The immunoglobulin-like superfamily member IGSF3 is a developmentally regulated protein that controls neuronal morphogenesis. *Dev. Neurobiol.* **77**, 75–92 (2017).
24. Huang, Z.-X. *et al.* The Male Abnormal Gene Family 21 (Mab21) Members Regulate Eye Development. *Curr. Mol. Med.* (2016) doi:10.2174/1566524016666160824150729.
25. Binder, C. *et al.* CD2 Immunobiology. *Frontiers in Immunology* (2020) doi:10.3389/fimmu.2020.01090.
26. Sawcer, S. *et al.* Genetic risk and a primary role for cell-mediated immune mechanisms in multiple sclerosis. *Nature* (2011) doi:10.1038/nature10251.
27. Lonsdale, J. *et al.* The Genotype-Tissue Expression (GTEx) project. *Nature Genetics* (2013) doi:10.1038/ng.2653.
28. Edgar, R., Domrachev, M. & Lash, A. E. Gene Expression Omnibus: NCBI gene expression and hybridization array data repository. *Nucleic Acids Res.* (2002).
29. Oki, S. *et al.* Ch IP -Atlas: a data-mining suite powered by full integration of public Ch IP -seq data. *EMBO Rep.* (2018) doi:10.15252/embr.201846255.
30. Lo, D. J. *et al.* Selective targeting of human alloresponsive CD8 + effector memory T cells based on CD2 expression. *Am. J. Transplant.* (2011) doi:10.1111/j.1600-6143.2010.03317.x.
31. Arnold, A. P. Conceptual frameworks and mouse models for studying sex differences in physiology and disease: Why compensation changes the game. *Experimental Neurology* (2014) doi:10.1016/j.expneurol.2014.01.021.
32. Oliva, M. *et al.* The impact of sex on gene expression across human tissues. *Science* (2020) doi:10.1126/science.aba3066.
33. Burton, P. R. *et al.* Association scan of 14,500 nonsynonymous SNPs in four diseases identifies autoimmunity variants. *Nat. Genet.* (2007) doi:10.1038/ng.2007.17.
34. Browning, B. L. *et al.* Gender-stratified analysis of DLG5 R30Q in 4707 patients with Crohn disease and 4973 controls from 12 Caucasian cohorts. *J. Med. Genet.* (2008) doi:10.1136/jmg.2007.050773.
35. Mersha, T. B. *et al.* Genomic architecture of asthma differs by sex. *Genomics* (2015) doi:10.1016/j.ygeno.2015.03.003.

36. Binder, C., Sellberg, F., Cvetkovski, F., Berglund, E. & Berglund, D. Siplizumab, an Anti-CD2 Monoclonal Antibody, Induces a Unique Set of Immune Modulatory Effects Compared to Alemtuzumab and Rabbit Anti-Thymocyte Globulin In Vitro. *Front. Immunol.* (2020) doi:10.3389/fimmu.2020.592553.
37. Rostaing, L. *et al.* Alefacept combined with tacrolimus, mycophenolate mofetil and steroids in de novo kidney transplantation: A randomized controlled trial. *Am. J. Transplant.* (2013) doi:10.1111/ajt.12303.
38. Demetriou, P. *et al.* A dynamic CD2-rich compartment at the outer edge of the immunological synapse boosts and integrates signals. *Nat. Immunol.* (2020) doi:10.1038/s41590-020-0770-x.
39. Orlik, C. *et al.* Keratinocytes costimulate naive human T cells via CD2: a potential target to prevent the development of proinflammatory Th1 cells in the skin. *Cell. Mol. Immunol.* (2019) doi:10.1038/s41423-019-0261-x.
40. Suthanthiran, M. T-cell differentiation antigen cluster 2 (CD2) is a receptor for accessory cells and can generate and/or transduce accessory signals. *Cell. Immunol.* (1988) doi:10.1016/0008-8749(88)90280-8.
41. Koyasu, S. *et al.* Role of interaction of CD2 molecules with lymphocyte function-associated antigen 3 in T-cell recognition of nominal antigen. *Proc. Natl. Acad. Sci. U. S. A.* (1990) doi:10.1073/pnas.87.7.2603.
42. Killeen, N., Stuart, S. G. & Littman, D. R. Development and function of T cells in mice with a disrupted CD2 gene. *EMBO J.* (1992) doi:10.1002/j.1460-2075.1992.tb05532.x.
43. Kyewski, B. A. *et al.* The effects of anti-CD2 antibodies on the differentiation of mouse thymocytes. *Eur. J. Immunol.* (1989) doi:10.1002/eji.1830190526.
44. Teh, S. J., Killeen, N., Tarakhovsky, A., Littman, D. R. & Teh, H. S. CD2 regulates the positive selection and function of antigen-specific CD4-CD8 + T cells. *Blood* (1997) doi:10.1182/blood.v89.4.1308.
45. Sasada, T. & Reinherz, E. L. A critical role for CD2 in both thymic selection events and mature T cell function. *J. Immunol.* **166**, 2394–403 (2001).
46. Gokhale, A., Kanthala, S., Latendresse, J., Taneja, V. & Satyanarayanajois, S. Immunosuppression by Co-stimulatory Molecules: Inhibition of CD2-CD48/CD58 Interaction by Peptides from CD2 to Suppress Progression of Collagen-induced Arthritis in Mice. *Chem. Biol. Drug Des.* **82**, 106–118 (2013).
47. Wakkach, A., Cottrez, F. & Groux, H. Differentiation of regulatory T cells 1 is induced by CD2 costimulation. *J. Immunol.* **167**, 3107–13 (2001).
48. Podesta, M. A. *et al.* Siplizumab selectively depletes effector memory T-cells and promotes a relative expansion of alloreactive regulatory T-cells in vitro. *Am. J. Transplant* (2019) doi:10.1111/ajt.15533.
49. Gottlieb, A. B. Alefacept for psoriasis and psoriatic arthritis. in *Annals of the Rheumatic Diseases* (2005). doi:10.1136/ard.2005.042655.
50. McKinney, E. F., Lee, J. C., Jayne, D. R. W., Lyons, P. A. & Smith, K. G. C. T-cell exhaustion, co-stimulation and clinical outcome in autoimmunity and infection. *Nature* **523**, 612–616 (2015).

51. Diggins, K. E. *et al.* Exhausted-like CD8 T cell phenotypes linked to C-peptide preservation in alefacept-treated T1D subjects. *JCI Insight* (2020) doi:10.1172/jci.insight.142680.
52. Fink, A. L. & Klein, S. L. The evolution of greater humoral immunity in females than males: implications for vaccine efficacy. *Current Opinion in Physiology* (2018) doi:10.1016/j.cophys.2018.03.010.
53. CONFAVREUX, C., HUTCHINSON, M., HOURS, M. M., CORTINOVIS-TOURNIAIRE, P. & MOREAU, T. Rate of Pregnancy-Related Relapse in Multiple Sclerosis. *Surv. Anesthesiol.* (1999) doi:10.1097/00132586-199902000-00027.
54. Ahlqvist, E. *et al.* High-resolution mapping of a complex disease, a model for rheumatoid arthritis, using heterogeneous stock mice. *Hum. Mol. Genet.* **20**, 3031–3041 (2011).
55. Livak, K. J. & Schmittgen, T. D. Analysis of Relative Gene Expression Data Using Real-Time Quantitative PCR and the 2 − ΔΔCT Method. *Methods* **25**, 402–408 (2001).
56. Tantin, D., Voth, W. P. & Shakya, A. Efficient Chromatin Immunoprecipitation using Limiting Amounts of Biomass. *J. Vis. Exp.* e50064–e50064 (2013) doi:10.3791/50064.
57. Holmdahl, R. *et al.* Genetic analysis of murine models for rheumatoid arthritis. *Hum. Genome Methods* (1998).
58. Abdul-Majid, K.-B. *et al.* Screening of several H-2 congenic mouse strains identified H-2q mice as highly susceptible to MOG-induced EAE with minimal adjuvant requirement. *J. Neuroimmunol.* **111**, 23–33 (2000).
59. Dumas, J., Gargano, M. A. & Dancik, G. M. ShinyGEO: A web-based application for analyzing gene expression omnibus datasets. *Bioinformatics* (2016) doi:10.1093/bioinformatics/btw519.
60. Perez-Riverol, Y. *et al.* The PRIDE database and related tools and resources in 2019: Improving support for quantification data. *Nucleic Acids Res.* (2019) doi:10.1093/nar/gky1106.
61. Zheng, R. *et al.* Cistrome Data Browser: Expanded datasets and new tools for gene regulatory analysis. *Nucleic Acids Res.* (2019) doi:10.1093/nar/gky1094.
62. Fornes, O. *et al.* JASPAR 2020: Update of the open-Access database of transcription factor binding profiles. *Nucleic Acids Res.* (2020) doi:10.1093/nar/gkz1001.

Figures

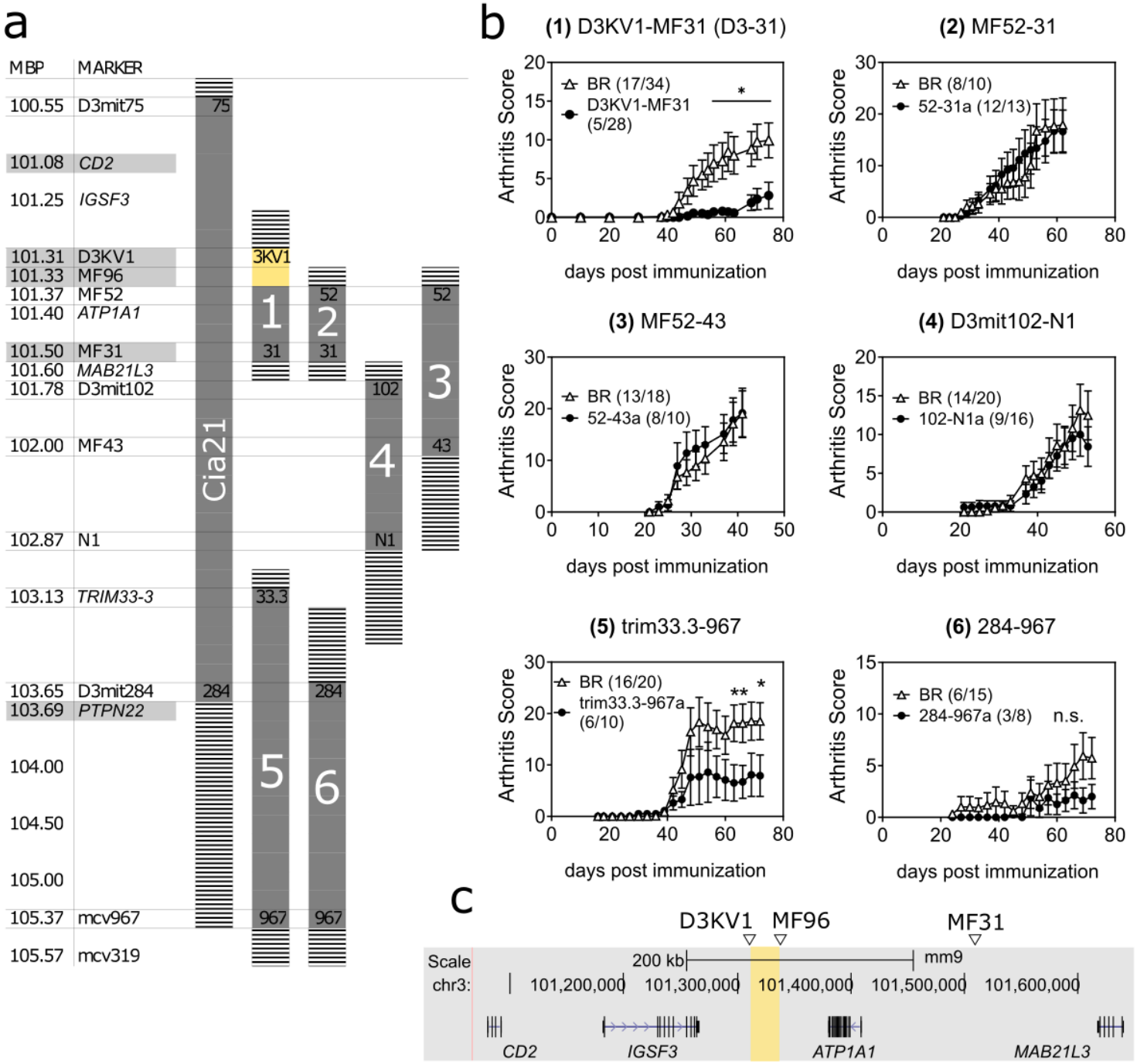

Figure 1

Schematic representation of Cia21 and phenotype driving D3KV1-MF31 (D3-31) recombinant fragment. The Cia21 QTL resulted from an inter-cross between the CIA susceptible C57BL/10.RII (BR) and the CIA resistant RIIIS/J (R3) strains. Cia21 is present on chromosome 3 qF2.2 and is 3 Mbp in size. a) Schematic representation of the Cia21 QTL and recombinant mice derived by intercrossing of Cia21 heterozygotes. Important genetic markers and genes are indicated on the left. The critical D3KV1-MF96 interval is highlighted in yellow. Uncertainty borders are dashed. b) Collagen-induced arthritis in female recombinant mice from (a) compared to BR littermate controls. Incidence and total number of mice are indicated in parenthesis on the respective graphs. Data are summarized as mean (SEM). c) Detailed view

of D3KV1-MF31 (fragment 1) and close-by genes. The critical D3KV1-MF96 interval is highlighted in yellow. Coordinates according to mouse NCBI37/mm9 build. n.s., not significant; *, $p < 0.05$; **, $p < 0.01$.

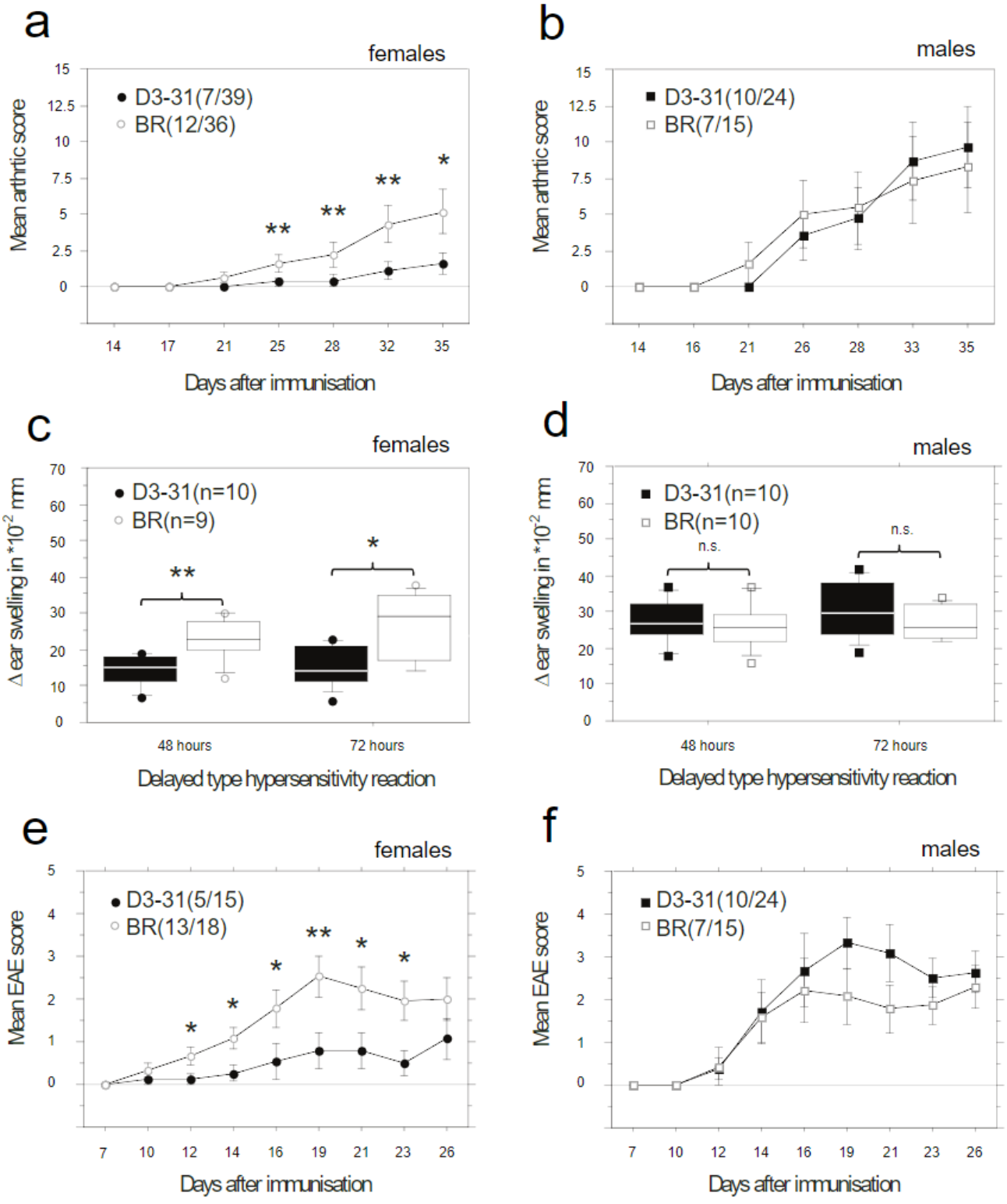

Figure 2

D3-31 mice are protected from several models of T cell-dependent autoimmunity in a sex-specific manner. Collagen-induced arthritis (CIA) in a) female and b) male BR and D3-31 mice. Delayed-type hypersensitivity (DTH) reaction in c) female and d) male BR and D3-31 mice. MBP89-101-induced

experimental autoimmune encephalomyelitis (EAE) in e) female and f) male BR and D3-31 mice. Incidence and total number of mice used are indicated in parenthesis. Data are summarized as mean (SEM). *, $p < 0.05$; **, $p < 0.01$.

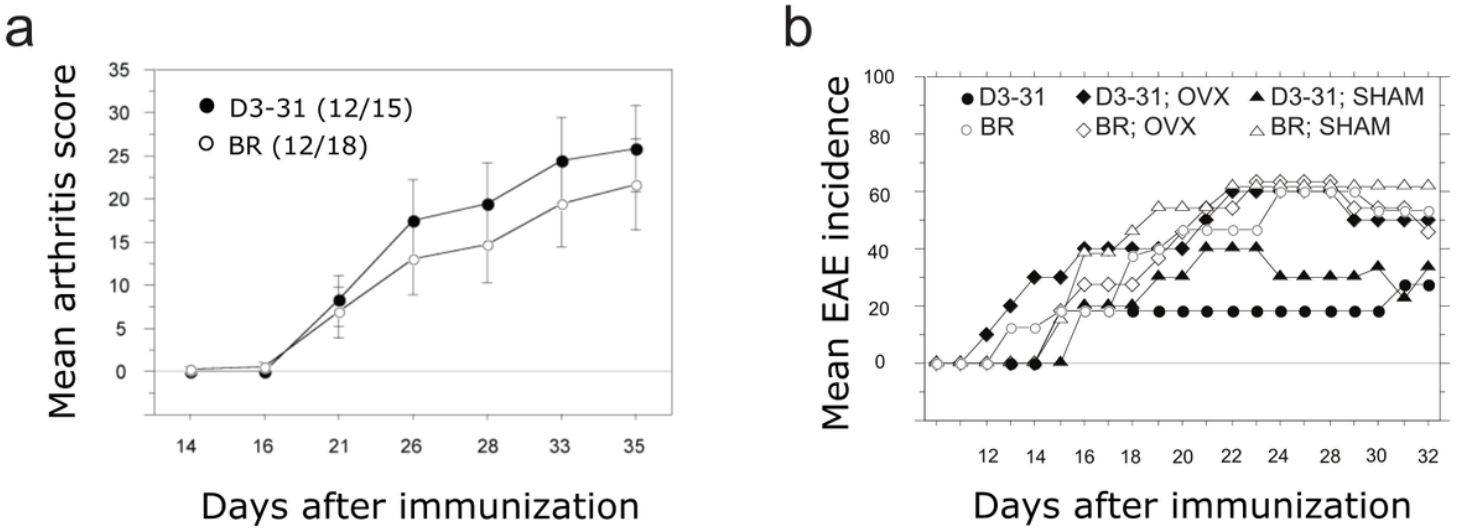

c

	Surgery	Day of onset (mean±SEM)	Incidence of EAE	Maximal EAE score (mean±SEM)	Accumulated EAE severity (mean±SEM)
D3-31	-	22±2	4/16	0.6±0.2	5.3±2.0
BR	-	20±1	12/22	1.7±0.3*	15.9±3.3*
D3-31	SHAM	21±3	5/16	0.6±0.2	5.5±2.6
BR	SHAM	19±1	11/22	1.9±0.5	18.6±5.1
D3-31	OVX	17±1	10/18	2.2±0.5	20.0±5.0
BR	OVX	19±1	13/20	2.6±0.5	23.5±5.7

Figure 3

Female sex hormones are required for the protective phenotype in D3-31 mice. a) CIA severity and incidence (in parenthesis) in ovariectomized D3-31 and BR mice. b) Incidence of EAE in ovariectomized (OVX) and sham operated (SHAM) D3-31 and BR mice. c) Table comparing incidence, maximal score and accumulated severity of EAE experiment shown in (b). Data are summarized as mean (SEM). *, $p < 0.05$.

a

ID	Position chr3:	BR>R3
1	101310478-479	A > G (D3KV1), SNP478
1	101310479-480	C > G (D3KV1), SNP478
2	101333185-186	A > G
3	101337088-269	(TCTCC)n; (MF96)
4	101354253-493	MER1 type repeat (MF52)

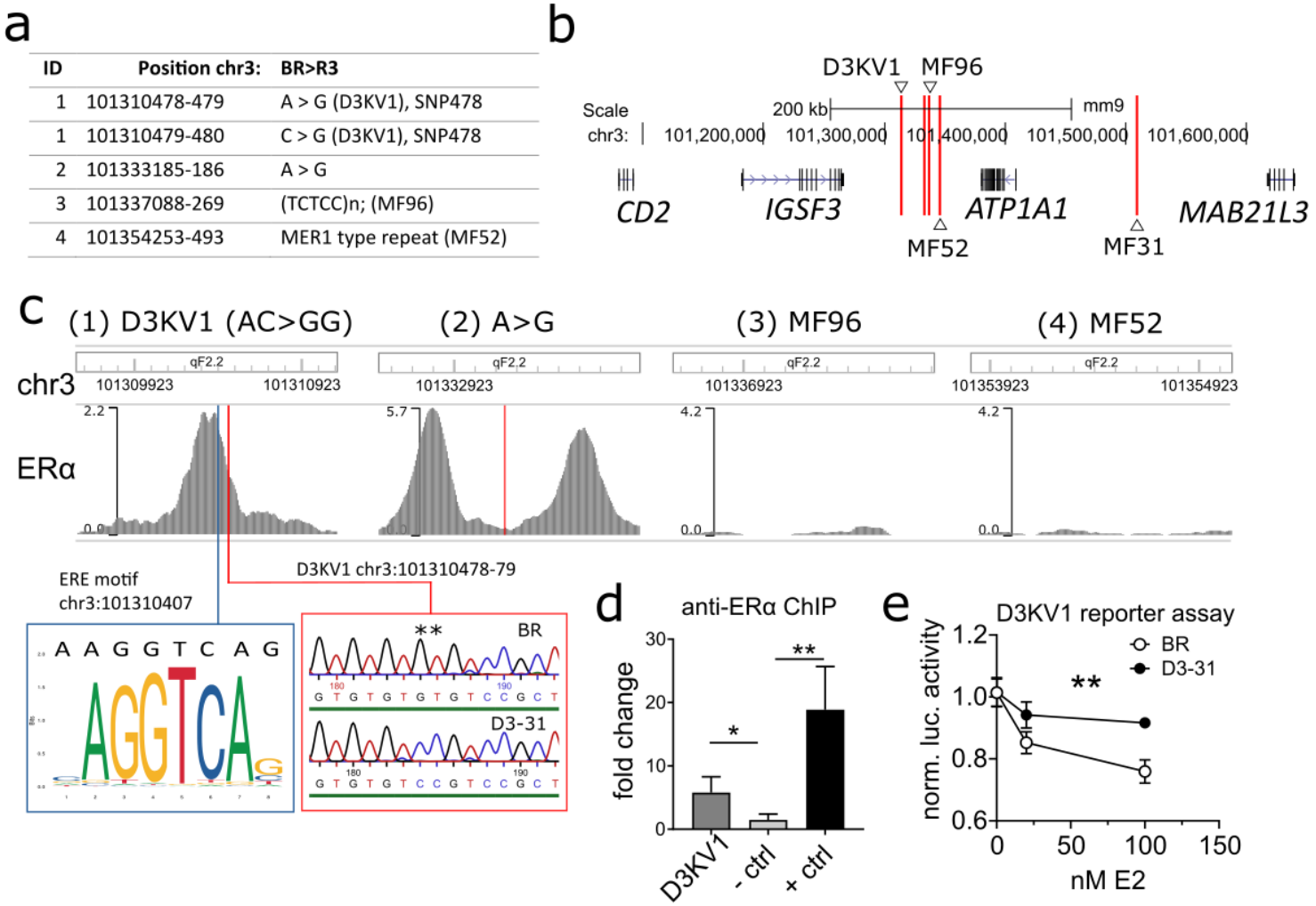

Figure 4

Polymorphism in D3-31 estrogen receptor binding site affects E2-mediated transcriptional activity. a) Sequencing results showing genetic variants within critical D3KV1-MF96 interval. b) Detailed schematic overview of polymorphisms (denoted by red lines) in the D3KV1-MF96 interval. SNP478 denotes a AC > GG substitution on chr3:101310478-79. c) ChIP-seq data from mouse uterus (extracted from GSM894054 61) showing ERα binding intensity to polymorphic regions listed in (a). Consensus ER binding motif (UN0308.1 62) and SNP478 are highlighted in blue and red, respectively. Coordinates according to mouse NCBI37/mm9 build. d) Rabbit anti-mouse ERα ChIP-qPCR data confirming binding of ERα to SNP478 in spleen cells. A gene dessert was used as negative control (-ctrl) and a known ERα binding site (CSF2RA 29) as positive control (+ ctrl). Values are expressed as fold enrichment over rabbit IgG mock IP (n=5/group). e) Effect of SNP478 on the transcriptional activity of the D3KV1 ERα binding site shown in (c). The candidate ERα binding site (chr3:101310478 ± 100 bp to each side) was cloned in its two variant forms (AC and GG) into luciferase reporter constructs. The constructs were transfected into MCF7 cells to evaluate transcriptional activity (n=5/group). Data are summarized as mean (SEM). *, $p < 0.05$; **, $p < 0.01$.

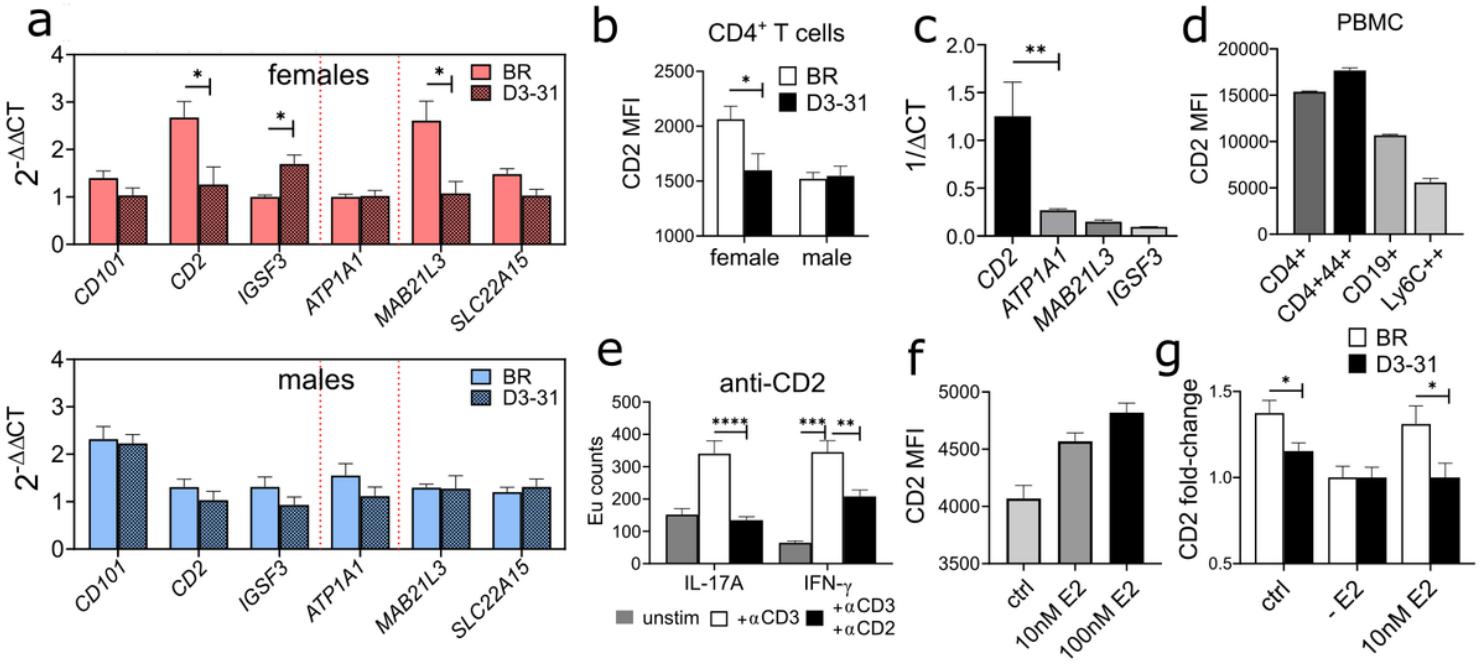

Figure 5

D3-31 mice show sex-specific differences in CD2 expression. a) Expression of genes surrounding the D3-31 congenic fragment in lymph nodes cells. Dotted lines indicate fragment borders. Expression in female and male mice is shown in red and blue, respectively. b) CD2 protein expression in lymph node CD4+ T cells from female and male D3-31 and BR mice (flow cytometry). c) Expression of CD2 and other surrounding genes in lymph nodes from BR mice. d) CD2 protein expression in blood circulating T cells, B cells, and monocytes (flow cytometry). e) Secretion of IL-17A and IFN-γ in T cells stimulated with anti-CD3 mAb only, or anti-CD3 and anti-CD2 mAb. f) CD2 expression in lymph node T cells after in vitro culturing with increasing concentrations of 17-β-estradiol (E2). g) Comparison of CD2 expression in T cells from D3-31 and BR mice cultured in normal medium (ctrl), medium (charcoal) stripped of E2 (-E2), or -E2 medium supplemented with 10 nM E2. Data are summarized as mean (SEM) from n=5 mice per group. *, $p < 0.05$; **, $p < 0.01$.

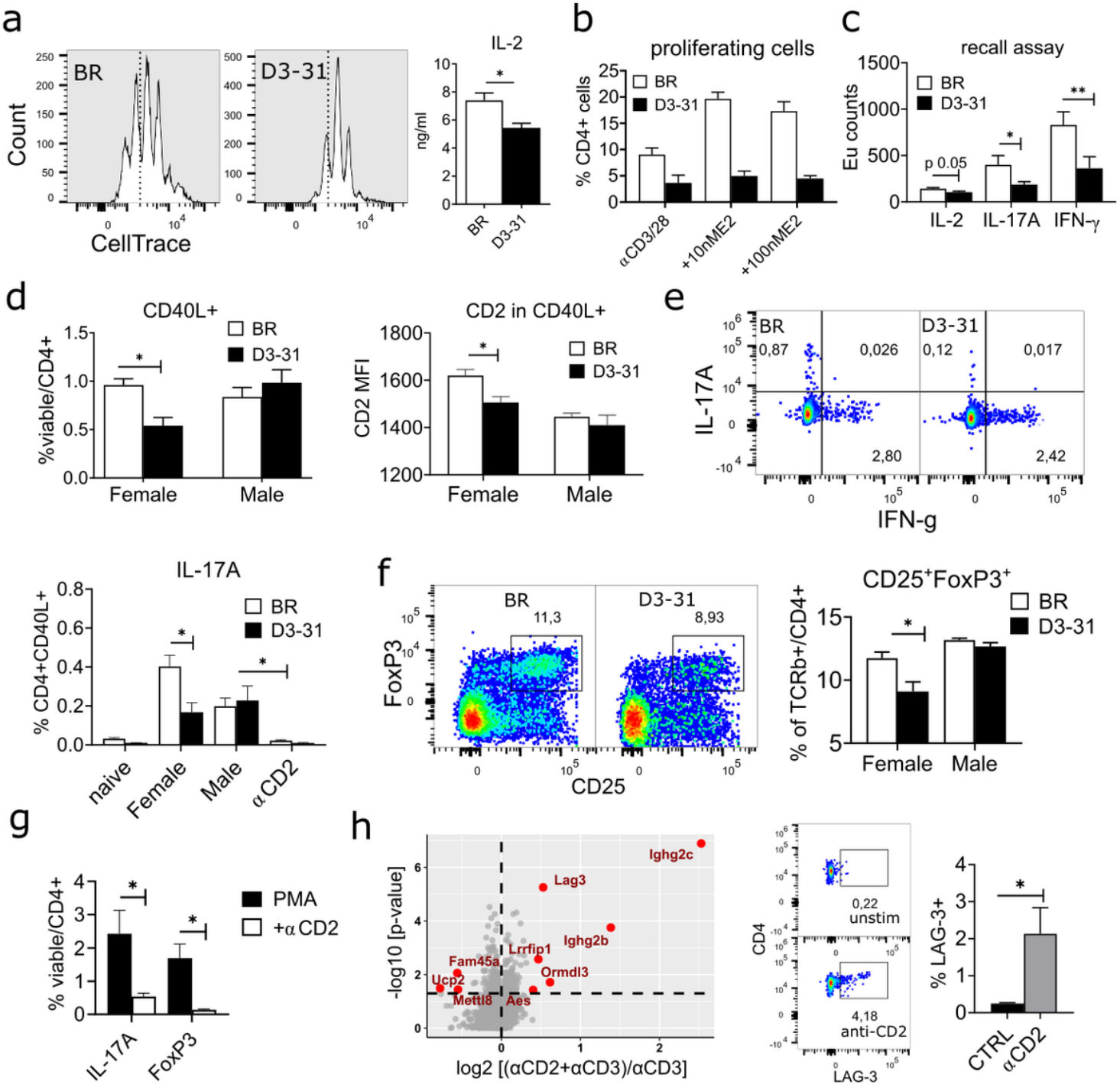

Figure 6

Sex-specific differences in CD2 expression limit the T cell responses in female D3-31 mice. a) Proliferation and IL-2 secretion of CD4+ lymph node T cells after stimulation with anti-CD3/anti-CD28 mAbs. b) Proliferation of BR and D3-31 CD4+ T cells as in (a) in the presence of increasing concentrations of E2 (10-100 nM). c) Antigen recall assay showing proinflammatory cytokine secretion by lymph node cell cultures from CIA mice after recall with bovine collagen type II (bCII). Lymph nodes were harvested 10 days after immunization with bCII (day 10). d) Quantification of antigen experienced CD40L+CD4+ T cells in lymph nodes from CIA mice (day 10), and expression of CD2 in these cells. e)

Gating and quantification of IL-17A+CD40L+ T cells in lymph nodes from CIA mice (day 10). Cells were restimulated ex vivo with PMA in the presence or absence of anti-CD2 mAb before staining for flow cytometry. f) Gating and quantification of CD25+FOXP3+Tregs in lymph nodes from CIA mice (day 10). g) Expression of IL-17A and FOXP3 in CD4+ naïve T cells stimulated with PMA in the absence or presence of anti-CD2 mAb. h) Volcano plot comparing the proteomic profile of CD4+ T cells stimulated with anti-CD3 mAb in the presence and absence of anti-CD2 mAb (left). Flow cytometry data showing LAG-3 expression in CD4+ T cells after culture with anti-CD2 mAb (right). Data are summarized as mean (SEM) from n=5 mice per group. *, p < 0.05; **, p < 0.01.

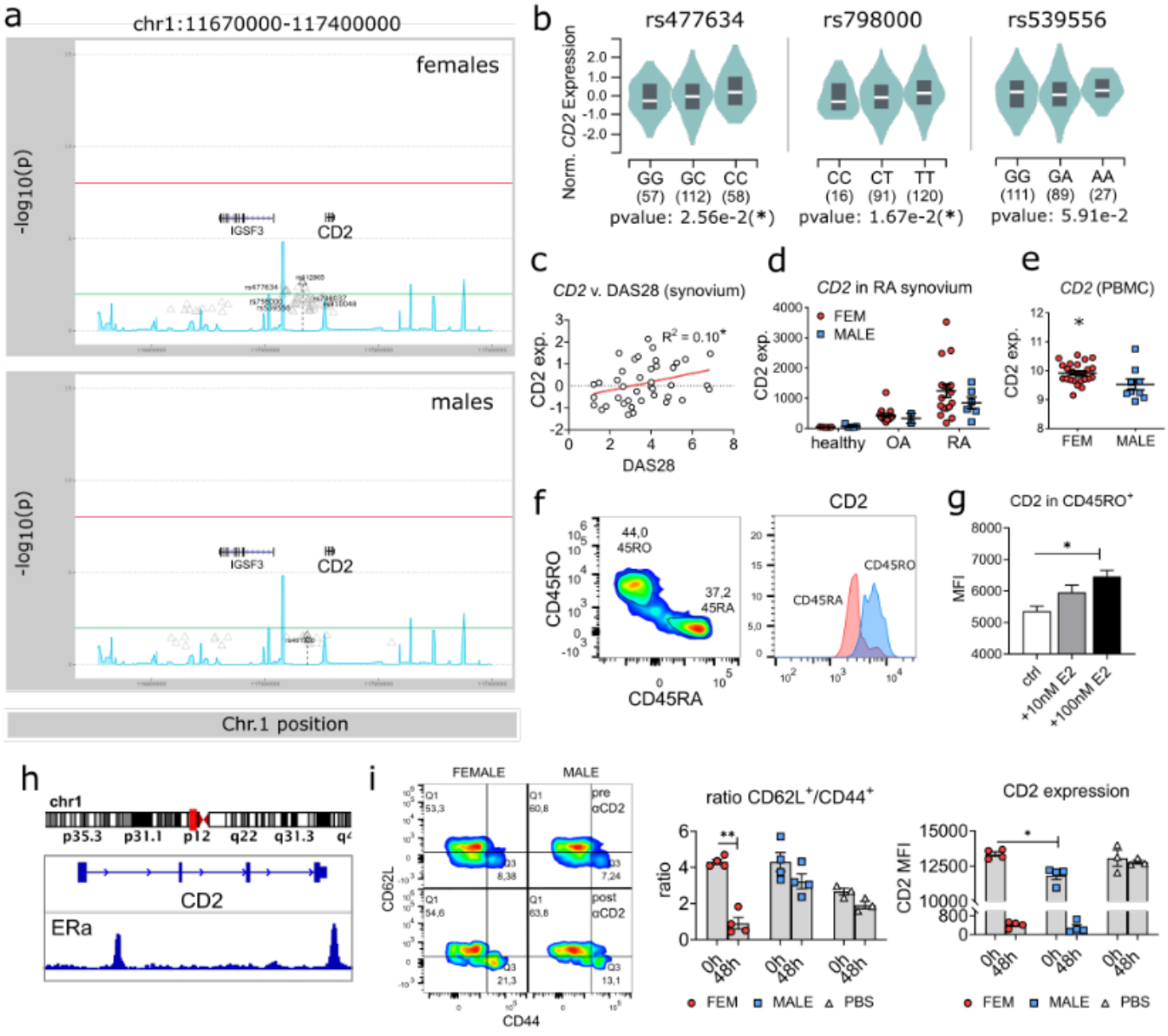

Figure 7

E2-mediated regulation of CD2 is conserved in humans. a) Genetic association data showing association between CD2 polymorphisms and rheumatoid arthritis (RA) in female (top) and male (bottom) patients

(EIRA cohort, 1341 males and 3361 females). b) Effect of indicated SNPs on expression of CD2 in human spleen as determined using GTEx 32. c) CD2 expression in synovia from RA patients plotted against disease activity (DAS28-CRP). Data was extracted from GEO Dataset GSE45867. d) Expression of CD2 in synovial tissue from RA patients, osteoarthritis (OA) patients, or healthy controls (GEO GDS5401-3). Females are shown in red and males in blue. e) Expression of CD2 in PBMCs from healthy males and females (GEO GDS5363). f) CD2 expression on antigen experienced CD45RO+ or naïve CD45RA+ CD4+ T cells from blood of a healthy donor. g) CD2 expression in CD45RO+ T cells after 24h incubation with 10-100 nM E2 (n=3/group). h) Anti-ERα ChIP-seq data showing binding of ERα to the human CD2 locus in MCF7 cell line (extracted from 29, SRX1995230). i) Naïve BR male and female mice were injected i.p. with 50 µg anti-CD2 mAb (RM2-5). Circulating CD4+ T cells were analysed before (0 h) and 48 h after mAb injection. Ratio of naive (CD62L+) to effector (CD44+) CD4+ T cells (left), and CD2 expression in CD4+ T cells (right). Data are expressed as mean (SEM). *, $p < 0.05$; **, $p < 0.01$.

Supplementary Files

This is a list of supplementary files associated with this preprint. Click to download.

- NCOMMS2110552.pdf
- SupplementaryMaterials.docx